DYRK1A binds to an evolutionarily conserved WD40-repeat protein WDR68 and induces its nuclear translocation

Yoshihiko Miyata*, Eisuke Nishida

Department of Cell and Developmental Biology, Graduate School of Biostudies, Kyoto University, Kitashirakawa Oiwake-cho, Kyoto 606-8502, Japan

*** Corresponding author.** Department of Cell & Developmental Biology, Graduate School of Biostudies, Kyoto University, Kitashirakawa Oiwake-cho, Sakyo-ku, Kyoto 606-8502, Japan.

Tel.: +81-75-753-4231; fax: +81-75-753-4235.

E-mail address: ymiyata@lif.kyoto-u.ac.jp (Y. Miyata).

ABSTRACT

DYRK1A is encoded in the Down's syndrome critical region on human chromosome 21, and plays an important role in the functional and developmental regulation of many types of cells, including neuronal cells. Here we have identified WDR68, an evolutionarily conserved protein with WD40-repeat domains, as a cellular binding partner of DYRK1A. WDR68 was originally identified in petunia as AN11 that controls the pigmentation of flowers by stimulating the transcription of anthocyanin biosynthetic genes. Experiments with RNA interference showed that WDR68 was indispensable for the optimal proliferation and survival of mammalian cultured cell, and WDR68 depletion induced cell apoptosis. DYRK1A and DYRK1B, but not DYRK2, DYRK3, or DYRK4, bound to endogenous and expressed WDR68. The N-terminal domain, but not the catalytic kinase domain or the C-terminal domain of DYRK1A, was responsible for the WDR68 binding. Deletions in the N-terminal or C-terminal region outside of the central WD40-repeats of WDR68 abolished its binding to DYRK1A, suggesting that WD40 repeats are not sufficient for the association with DYRK1A. Immunofluorescent staining revealed that WDR68 was distributed throughout the cell. Importantly, nuclear accumulation of WDR68 was observed upon co-expression of the wild type and a kinase-dead mutant of DYRK1A. Taken together, these results suggest that DYRK1A binds specifically to WDR68 in cells, and that the binding, but not the phosphorylation event, induces the nuclear translocation of WDR68.

Keywords:

DYRK1A

WDR68

WD40-repeat

Down's syndrome

Nuclear translocation

Abbreviations

DYRK, dual-specificity tyrosine-phosphorylation regulated protein kinase / dual-specificity YAK1-related protein kinase; WDR, WD repeat; Hsp, heat shock protein; PARP, poly-ADP ribose polymerase.

1. Introduction

DYRK (Dual-specificity tYrosine-phosphorylation Regulated protein Kinase/Dual-specificity YAK1-Related protein Kinase) is a family of mammalian protein kinases, including five members; DYRK1A, DYRK1B, DYRK2, DYRK3, and DYRK4 [1, 2]. Each member of DYRKs has a mutually homologous (43-85% identities) catalytic domain in the middle of the amino acid sequence with more diverged N- and C-terminal extensions. The amino acid sequences of the catalytic domains of DYRKs are similar to those of MAP kinases [3], suggesting that DYRKs might play a role in cellular signal transduction system. For activation, MAP kinases should be phosphorylated on both threonine and tyrosine residues in the activation loop region by upstream MAP kinase kinases, while DYRKs phosphorylate themselves on an intramolecular tyrosine residue in the activation loop for correct folding, maturation, and kinase activity [4, 5]. DYRK1A is expressed ubiquitously, whereas other members of DYRKs are expressed in a tissue-specific manner [2], suggesting that each member of DYRKs has its own specialized function by interacting with a different set of protein partners.

A human gene for DYRK1A has been received considerable attention because DYRK1A is encoded in the Down's syndrome critical region in chromosome 21 [6, 7]. Indeed, overexpression of DYRK1A is suggested to be responsible for a part of Down's syndrome phenotypes [8-12]. DYRK1A phosphorylates NFAT (Nuclear Factor of Activated T cells) and dysregulates NFAT by counteracting calcineurin-dependent dephosphorylation of NFAT which is prerequisite for the nuclear translocation and activation of NFAT [13, 14]. NFAT dysregulation is suggested to be a part of the molecular mechanisms for developmental abnormalities in Down's syndrome patients [13]. DYRK1A has been reported to phosphorylate many physiologically important substrates, including tau

protein [10, 11, 15], glycogen synthase [16], CRY2 [17], and caspase-9 [18, 19], however, the precise mechanism how the modest overexpression of DYRK1A by chromosome 21 trisomy induces pleiotropic physiological results remains obscure.

The kinase catalytic domain of DYRK1B is 85% identical with that of DYRK1A, and in the N-terminal domain there is a region with 80 amino acids where the sequence identity is 71% between DYRK1A and DYRK1B. By contrast, the C-terminal regions of these kinases differ exceedingly both in their lengths and sequences [20]. While DYRK1A is ubiquitously expressed and predominant in the brain, DYRK1B is mainly expressed in muscle and testis [20]. DYRK1B plays a critical role in muscle differentiation [21] and transmits cell survival signals [22, 23]. In addition, DYRK1B is a downstream effector of oncogenic K-ras [24] and mediates some of the ras-activated signaling [25], suggesting a role for DYRK1B in tumor progression.

WDR68 (WD-repeat protein 68) was originally identified in petunia as a gene (AN11) responsible in a locus that controls the pigmentation of flowers by stimulating the transcription of anthocyanin biosynthetic genes [26]. Evolutionarily conserved orthologs have been identified in many other species, including human that do not produce anthocyanin [26]. The amino acid sequence of human AN11 (HAN11) is 100% identical with that of monkey, mouse, rat, dog, cow, and even chicken. The human AN11 has 52% amino acid identity with petunia AN11 and partially complements the an11 petunia mutant, showing the functional conservation [26]. AN11 and its orthologs all encode a protein with five WD40-repeats and are therefore termed collectively as WDR68. WDR68 is also referred as DCAF7, one of Ddb1- and Cul4-associated factors [27]. In general, WD40 domains are believed to facilitate interaction with other proteins, consistent with the observation that many of WD40-repeat proteins are found in multi-protein complexes [28, 29]. All the evidence suggests that WDR68 plays a fundamental role in many species from plants to mammals, probably by

protein-protein interactions, although biochemical and physiological function of WDR68 remains to be elucidated.

Two previous reports implicated a functional relationship between WDR68 and DYRK1A. Skurat *et al*. biochemically followed a kinase activity that phosphorylates Ser640 of glycogen synthase, and identified this kinase activity as a mixture containing a short DYRK1A fragment and WDR68 [16]. GLI1 is a transcription factor involved in the Hedgehog pathway and is phosphorylated and positively regulated by DYRK1A [30]. Morita *et al*. reported that WDR68 overexpression repressed DYRK1A-dependent GLI1 transcriptional activity [31]. It should be of biochemical and physiological importance to examine the interaction between DYRK1A and WDR68 at a molecular level to unveil physiological functions of DYRK1A and WDR68.

In this report, we identified WDR68 as a major cellular binding partner of DYRK1A. WDR68 bound to DYRK1A and DYRK1B, but not to DYRK2, DYRK3, or DYRK4. We have newly established that WDR68 is essential for the cell proliferation and survival. WDR68 was distributed throughout the cell, and the binding of DYRK1A to WDR68 induced nuclear translocation of WDR68. Based on these results, physiological importance of the association between DYRK1A and WDR68 is discussed.

2. Materials and methods

2.1. Reagents and antibodies

Anti-FLAG antibody (M2), HRP-conjugated anti-FLAG antibody, and anti-FLAG-affinity resin were from Sigma. HRP-conjugated anti-HA (12CA5) and anti-Cdc37 (E-4) antibodies were from Roche and Santa Cruz, respectively. Rabbit polyclonal antibody specific for caspase-cleaved form of

PARP (Asp214) was from Cell Signaling Technology. Anti-Hsp90 (Heat Shock Protein 90) antibody was described previously [32, 33]. Non-immune rabbit IgG for negative control experiments was from SantaCruz. An antibody specific for WDR68 was raised in rabbits against a peptide, CEDPILAYTAEGEINN, corresponding to amino acids 304-318 of human WDR68 with an additional N-terminal Cys for conjugation. The antiserum was purified on an affinity resin conjugated with the antigen peptide. The peptide synthesis, immunization, and affinity purification were performed at SCRUM Inc. (Tokyo, Japan). Hoechst 33342 was from Sigma.

pEGFP-C1 from Clontech was mutagenized *in vitro* by PCR with mutagenic primers (sense sequence = 5′-CGACGGTACC*GCGGCCGC*GGGATCCACC-3′). This mutation introduced a new in-frame *Not* I site in the multi-cloning site of the vector between *Sac* II and *BamH* I sites. The nucleotide sequence of an *Nhe* I-*BamH* I fragment of the mutagenized plasmid was confirmed by direct sequencing and the *Nhe* I-*BamH* I region of parental pEGFP-C1 vector was substituted by the mutagenized *Nhe* I-*BamH* I fragment. Obtained mutagenized vector with the *Not* I cloning site was referred as pEGFP-C1Not hereafter.

2.2. Molecular cloning of human DYRK family protein kinases

cDNA fragments encoding full length human DYRK1A, DYRK1B, DYRK2, DYRK3, and DYRK4 were cloned by nested PCR amplification using human cDNA library plasmid (Takara) as a template. The oligonucleotide primer sequences used were: DYRK1A: 1st PCR 5′-CCATCAGGATGATATGAGACTTGAAAG-3′ (5′ upstream) / 2nd PCR 5′-GATCGCGGCCGCAAAGAAGACGATGCATACAGGAGGAGA-3′ (*Not* I + 1st Met); DYRK1B: 1st PCR 5′-GGCCGGGCTCCCGCTCCAGGCCTCG-3′ (5′ upstream) / 2nd PCR 5′-GACTGCGGCCGCCATGGCCGTCCCACCGGGCCATG-3′ (*Not* I + 1st Met) and

5′-CAGTGCGGCCGCTCACGAGCTGGCTGCTGTGCTCT-3′ (3′ end + *Not* I, antisense); DYRK2: 1st PCR 5′-ACGGCAGCCCTGAAATGCATTTTCC-3′ (5′ upstream) / 2nd PCR 5′-GATTGCGGCCGCTAAGCACACAATGAATGATCACC-3′ (*Not* I + 1st Met) and 5′-GACGTGAGCTCAGCTAACAAGTTTTGG-3′ (3′ end antisense); DYRK3: 1st PCR 5′-ACCGGACCCCCAACTGGCGCCTCTC-3′ (5′ upstream) / 2nd PCR 5′-ATCGGCGGCCGCGATGGGAGGCACAGCTCGTGGGC-3′ (*Not* I + 1st Met) and 5′-GACTGCGGCCGCCTAGCTAATCAGTTTTGGCAATA-3′ (3′ end + *Not* I, antisense); DYRK4: 1st PCR 5′-CTGAAGTCATCCCTGCTGTATCAGG-3′ (5′ upstream) / 2nd PCR 5′-AGCTGCGGCCGCGATGCCGGCCTCAGAGCTCAAGG-3′ (*Not* I + 1st Met). The antisense primer sequence used in the 1st PCR (5′-CGGCTGGTTCTTTCCGCCTC-3′) is in the library vector (pAP3neo) region that was used for all of the cloning of DYRKs in common. For DYRK1A and DYRK4, an antisense primer (5′-CGGCTGGTTCTTTCCGCCTC-3′) downstream of a *Not* I site of the library vector was used in the 2nd PCR. As a result, the amplified PCR fragment of DYRK coding region contains a *Not* I site in 5′ upstream just before the starting ATG and another *Not* I site in the 3′ downstream of the stop codon. The whole coding regions of obtained PCR fragments were confirmed by direct sequencing. In the NCBI nucleotide database, 5, 3, 2, and 2 transcription variants are found for DYRK1A, DYRK1B, DYRK2, and DYRK3 respectively, and we obtained variant 1 (763 amino acids) for DYRK1A, variant b (589 amino acids) for DYRK1B, variant 1 (528 amino acids) for DYRK2, and variant 1 (588 amino acids) for DYRK3.

2.3. Molecular cloning of human WDR68

A cDNA fragment encoding full length human WDR68 was cloned by nested PCR amplification using human cDNA library plasmid (Takara) as a template. The oligonucleotide primer sequences

used are: 1st PCR 5′-CCACTGTTGACCCGGCCCGTACTGC-3′ (5′ upstream) and 5′-CGGCTGGTTCTTTCCGCCTC-3′ (pAP3neo, antisense) / 2nd PCR 5′-CGATGCGGCCGCCATGTCCCTGCACGGCAAACGGA-3′ (*Not* I + 1st Met) and 5′-GCATGCGGCCGCCTACACTCTGAGTATCTCCAGGC-3′ (3′ end + *Not* I, antisense). As a result, the amplified PCR fragment of WDR68 coding region contains a *Not* I site in the 5′ upstream just before the starting ATG and another *Not* I site in the 3′ downstream of the stop codon. The whole coding region was directly sequenced for confirmation.

2.4. Mammalian cell culture, transfection, cell extraction, and immunoprecipitation

COS7 cells were cultured and transfected with mammalian expression vectors by electroporation as described before [34, 35]. KB cells were cultured in DMEM supplemented with 10% FCS in humidified air containing 5% CO_2. Cells were washed with phosphate buffered saline and solubilized in IPW buffer (50 mM Tris-Cl, 50 mM NaCl, 100 mM NaF, 10 % glycerol, 2 mM EDTA, 2 mM sodium orthovanadate, 10 mM sodium pyrophosphate, 1 mM dithiothreitol, 1 % NP40, pH 8.0), supplemented with 1/100 (v/v) of a mammalian protease inhibitor cocktail (Nacalai Tesque, Kyoto Japan). The lysates were then centrifuged at 17,000 × g for 60 min at 2 °C and supernatants were recovered. Extracts with equal amounts of proteins were incubated with anti-FLAG agarose for 12 h at 4 °C. The immunocomplexes were extensively washed and analyzed as described previously [36, 37]. EZView Red protein G affinity gel (Sigma) was used for WDR68 immunoprecipitation.

2.5. A large-scale isolation and mass spectrometry analysis of DYRK1A-binding proteins

Lysate was prepared from 8 dishes (ϕ10 cm) of 3×FLAG-DYRK1A-transfected COS7 cells, mixed with 200 μL of anti-FLAG agarose for 6 h at 4 °C, and after extensive washing bound proteins were

eluted with 0.6 mg/ml of 3×FLAG peptide as described [36, 37]. Isolated proteins were concentrated by a Microcon Centrifugal Filter (10 kDa cut off) and analyzed by sodium dodecyl sulfate-polyacrylamide gel electrophoresis (SDS-PAGE) followed by CBB protein staining. A 42 kDa band was cut out from the gel, digested with trypsin, and analyzed by MALDI-TOF mass spectrometry at Shimadzu Biotech (Tsukuba, Japan) using Kratos Axima-CFRplus.

2.6. RNA interference experiments

"Stealth Select" siRNAs (HSS145522 and HSS145523) specific for human WDR68 were obtained from Invitrogen. Stealth RNAi Negative Control Medium GC Duplex (Invitrogen) was used as a control. siRNA transfection was performed using Lipofectamine RNAiMAX (Invitrogen) as described in a manufacturer's standard protocol with final 12 nM of siRNA. After indicated days, cells were washed with PBS and the numbers of attached cells were counted. Cell photos were taken with a phase contrast microscope (Zeiss Axiovert 200M). Cell extracts were prepared as described above and the accumulation of cleaved PARP as an apoptotic marker in the equal amount of proteins was examined by western blotting analysis.

2.7. Mutants of DYRK1A

For DYRK1A deletion mutants, following PCR primers were used to amplify the corresponding coding fragments. DYRK1A(N): 5′-GATCGCGGCCGCAAAGAAGACGATGCATACAGGAGGAGA-3′ and 5′-GCGGCCGCCTAACGATCCATCCACTTTTC-3′ (antisense) ; DYRK1A(K): 5′-GCGGCCGCGATGGATCGTTACGAAATTG-3′ and 5′-GCGGCCGCCTAGAAGAAACTGTGCTGCAGAG-3′ (antisense); DYRK1A(C):

5′-GCGGCCGCCATGAAAACAGCTGATGAAGGTA-3′ and 5′-GCGGCCGCTCACGAGCTAGCTACAGGAC-3′ (antisense); DYARK1A(N+K): 5′-GATCGCGGCCGCAAAGAAGACGATGCATACAGGAGGAGA-3′ and 5′-GCGGCCGCCTAGAAGAAACTGTGCTGCAGAG-3′ (antisense); DYRK1A(K+C): 5′-GCGGCCGCGATGGATCGTTACGAAATTG-3′ and 5′-GCGGCCGCTCACGAGCTAGCTACAGGAC-3′ (antisense). For the kinase-dead mutant of DYRK1A, two mutagenic primers 5′-GAATGGGTTGCCATCGATATAATAAAGAAC-3′ and 5′-GTTCTTTATTATATCGATGGCAACCCATTC-3′ (antisense) were used. Site-directed *in vitro* mutagenesis was performed essentially as described [35].

2.8. Deletion mutants of WDR68

Deletion mutants of WDR68 were produced by PCR amplification with following primers. Antisense primers used were WDR68(1-217): 5′-GCGGCCGCCTATTCGTAAATGATGGTGCTGTG-3′; WDR68(1-258): 5′-GCGGCCGCCTAAGGTGTGCAGGGAACCCGGAC-3′; WDR68(1-304): 5′-GCGGCCGCCTACTCAATGGCTCGGGGCATTTG-3′. A common sense primer 5′-CGATGCGGCCGCCATGTCCCTGCACGGCAAACGGA-3′ was used for these C-terminal deletion mutants. Sense primers used were WDR68(150-342): 5′-GCGGCCGCCATGGAGACAGGGCAGGTGTTAG-3′; WDR68(107-342): 5′-GCGGCCGCCATGGAGTGTTTGCTAAACAATA-3′; WDR68(55-342): 5′-GCGGCCGCCATGAGTTCAGAGTTTATTTGCAG-3′. A common antisense primer 5′-GCATGCGGCCGCCTACACTCTGAGTATCTCCAGGC-3′ was used for these N-terminal deletion mutants. For WDR68(55-304), primers 5′-GCGGCCGCCATGAGTTCAGAGTTTATTTGCAG-3′

(sense) and 5′-GCGGCCGCCTACTCAATGGCTCGGGGCATTTG-3′ (antisense) were used. All the coding regions of DYRK1A and WDR68 mutants were confirmed by direct sequencing.

2.9. Construction of mammalian expression vectors

The *Not* I fragments of DYRKs, DYRK1A mutants, WDR68, and its deletion mutants were ligated into the *Not* I site of p3×FLAG-CMV7.1 (Sigma), pEGFP-C1Not, and pcDNA3HA [35] to obtain mammalian expression plasmids encoding fusion proteins with 3×FLAG-, GFP-, and HA-tag, respectively.

2.10. Immunofluorescent staining

COS7 cells were transfected and immunostained essentially as described [38]. Alexa488- or Alexa546-conjugated secondary antibodies were used. Nuclear staining was performed by including Hoechst 33342 dye (1 μg/mL) in secondary antibody solutions. Fluorescent and phase contrast images of cells were obtained with immersion oil using a fluorescent microscope (Zeiss Axiophoto with Plan NEOFLUAR 40× lens).

2.11. Other procedures

SDS-PAGE was performed with 10% acrylamide gels. Silver staining of SDS-polyacrylamide gels was performed using 2D-Silver Stain II kit (Daiichi Pure Chemicals). Western blotting was performed using horseradish peroxidase-conjugated secondary antibodies (GE Healthcare Bio-sciences) or peroxidase-conjugated primary antibodies, and detection was performed using chemiluminescent system as described [37].

3. Results

3.1. Identification of a cellular DYRK1A-binding protein as an evolutionarily conserved WD40-repeat protein, WDR68

We searched for cellular binding partners of DYRK1A to understand a physiological role of DYRK family protein kinases at the molecular level. Cellular proteins bound to 3×FLAG-tagged DYRK1A were isolated and visualized by silver staining (Fig. 1A, *lane* 2). As a control, lysate from cells transfected with the empty vector was used (Fig. 1A, *lane* 1). As expected, 3×FLAG-DYRK1A was detected as an 89 kDa major band (Fig. 1A, *lane* 2). A 42 kDa binding protein (Fig. 1A, *lane* 2, *arrow*) was repeatedly detected in several independent experiments, which was not isolated in the control sample (Fig. 1A, *lane* 1). A large-scale isolation of the DYRK1A-associated proteins was then conducted, and the 42 kDa protein was analyzed by mass spectrometry. The obtained signals were searched for NCBInr database with taxonomy of metazoa and the top score (probability-based mowse score of 103) was obtained for gi|28913537. The protein was identified as WDR68, an evolutionarily conserved WD40-repeat protein with calculated molecular mass of 38,926. The number of mass values matched with peptide fragments was 17 and the sequence coverage was 56% (Fig. 1B). The result showed that DYRK1A makes a complex with WDR68 in cells. We made an antibody raised against a synthetic peptide corresponding to a C-terminal region of human WDR68. The sequence is 100% identical in WDR68 of human, monkey, mouse, cow, dog, chicken, zebrafish, and frog. The specificity of the antibody was examined by western blotting. As shown in Fig. 1C, the antibody recognized a single 42 kDa protein in COS7 cell lysate (*lane* 3). The antibody also recognized exogenously-expressed 3×FLAG-WDR68 in cell lysates (*lane* 4), while the preimmune serum showed no binding (Fig. 1C, *lanes* 1 & 2). These results showed that the anti-WDR68

antibody specifically recognizes endogenous and expressed WDR68.

3.2. WDR68 is essential for the optimal cell proliferation and survival

We then examined a physiological role for WDR68 by reducing intracellular levels of endogenous WDR68 by RNA interference experiments. Two independent specific siRNAs (RNAi-1 and RNAi-2) corresponding to the WDR68 mRNA sequence were introduced into mammalian cultured cells. 48 h after the transfection, the amounts of WDR68 in extracts of equal numbers of cells were examined by western blotting with the anti-WDR68 antibody (Fig. 2A, *upper panels*). In both COS7 (*left*) and KB cells (*right*), reduction in endogenous WDR68 was detected (*lanes* 2 & 3) as compared with cells transfected with a control siRNA (*lane* 1). The amounts of molecular chaperones Hsp90 (*left*) and Cdc37 (*right*) as control proteins were unchanged (Fig. 2A, *lower panels*). Cells were cultured in a normal medium and the numbers of living attached cells were counted everyday until day 7 after siRNA transfection. As shown in Fig. 2B, the proliferation of WDR68-reduced cells was severely suppressed after 2 days of siRNA introduction and the cells did not grow anymore after that, while the control cells continued to grow until day 3 when they reached full confluency. The microscopic observation of these cells showed that the reduction in WDR68 resulted in significant cell rounding and floating as compared with control cells (Fig. 2C). Almost the same results were obtained with KB cells (data not shown). We then examined if the depletion of endogenous WDR68 by siRNAs induced cell apoptosis. Cleavage of PARP by caspases has been widely accepted as a specific marker for cellular apoptotic process [39, 40]. As shown in Fig. 2D *upper panel*, we found that treatment of cells with the WDR68-specific siRNAs induced accumulation of caspase-cleaved PARP (*lanes* 6-8 & 10-12) while the control siRNA did not (*lanes* 1-4), indicating that cells underwent apoptotic process by the depletion of WDR68. The amounts of a control protein Hsp90 remained

unchanged (Fig. 2D, *lower panel*). The time course of the accumulation of caspase-cleaved PARP agreed well with that of the suppression of cell proliferation (Fig. 2B) and of appearance of rounding/floating cells (Fig. 2C). Taken together, these results indicated that WDR68 is essential for the optimal division, proliferation, and survival of cells, and the depletion of WDR68 suppress the cell proliferation by inducing cell apoptosis.

3.3. Co-immunoprecipitation of WDR68 with DYRK1A and DYRK1B

We then examined the binding between DYRK1A and WDR68 by co-expression experiments. COS7 cells were transfected with 3×FLAG-DYRK1A and HA-WDR68, then DYRK1A was immunoprecipitated with anti-FLAG antibody and WDR68 in the immunocomplexes was analyzed by western blotting with anti-HA antibody (Fig. 3A). WDR68 was co-immunoprecipitated with DYRK1A only when both proteins were co-expressed (Fig. 3A, *upper panel*, *lane* 3). Immunoprecipitates with a control antibody did not contain WDR68 (Fig. 3A, *upper panel*, *lanes* 4-6). In a reciprocal co-immunoprecipitation experiment, HA-DYRK1A was pulled down with isolated 3×FLAG-WDR68 when they were co-expressed (Fig. 3B, *upper panel*, *lane* 3). In both experiments, the expression levels of DYRK1A and WDR68 were shown by western blotting analysis with anti-HA and anti-FLAG antibodies (Fig. 3, *middle* and *lower panels*).

In the human genome, there encoded 5 members of DYRK family protein kinases, DYRK1A, DYRK1B, DYRK2, DYRK3, and DYRK4. We examined the binding of WDR68 to the 5 members of DYRKs by co-expression/co-immunoprecipitation experiments (Fig. 4A). Among 5 members of DYRKs, DYRK1A (*lane* 3) and DYRK1B (*lane* 4) were found to be associated with WDR68, but other DYRKs, DYRK2, DYRK3, and DYRK4, did not bind to WDR68 (*lanes* 5-7). In addition, we found that endogenous WDR68 was associated with immunoprecipitated DYRK1A and DYRK1B

(Fig. 4B, *lanes* 2 & 3). Sufficient amounts of all DYRKs were expressed with their expected molecular masses (Fig. 4C). These results showed that DYRK1A and DYRK1B, but not DYRK2, DYRK3, or DYRK4, bind to WDR68 in cells.

3.4. The N-terminal region of DYRK1A is essential for its binding to WDR68

DYRK1A is composed of three major domains, an N-terminal domain (N), the kinase catalytic domain (K) in the middle of the molecule, and a C-terminal tail (C) (Fig. 5A). The homology between DYRK1A and DYRK1B is highest in the kinase domain (85%), while the N-terminal and C-terminal domains contain less homologous regions (71% and 34%, respectively). To determine which part(s) of DYRK1A is responsible for the binding to WDR68, we made deletion mutants of DYRK1A and examined the binding of these mutants to WDR68 by co-immunoprecipitation experiments. As shown in Fig. 5B *top panel*, full length DYRK1A (*lane* 3) and the N-terminal domain of DYRK1A (*lane* 4), but not the kinase domain (*lane* 5) or the C-terminal tail of DYRK1A (*lane* 6), bound to WDR68. The essential role for the N-terminal region of DYRK1A in the WDR68 binding was further confirmed by another experiment. The results showed that a DYRK1A mutant lacking the C-terminal tail (DYRK1A(N+K)) (Fig. 5C, *upper panel*, *lane* 4) could bind to WDR68 as DYRK1A(N) (Fig. 5C, *upper panel*, *lane* 3), but a DYRK1A mutant lacking the N-terminal domain (DYRK1A(K+C)) (Fig. 5C, *upper panel*, *lane* 5) could not bind to WDR68. All the DYRK1A mutants were expressed and immunoprecipitated as polypeptides with expected molecular masses except DYRK1A(C) showing a slower mobility (42 kDa) than calculated molecular masses (30 kDa) (Fig. 5B & 5C, *middle panels*). Sufficient amounts of HA-WDR68 were expressed in all cases (Fig. 5B & 5C, *lower panels*). All these results indicated that the N-terminal domain of DYRK1A is essential and sufficient for the WDR68-binding. We then examined if the protein kinase activity of

DYRK1A is required for the binding to WDR68. We compared the binding of DYRK1A(WT) and DYRK1A(KD), a mutant without the kinase activity, to WDR68 by co-immunoprecipitation experiments. As shown in Figure 5D, both DYRK1A(WT) and DYRK1A(KD) bound equally well to WDR68, suggesting that the kinase activity is not required for the binding to WDR68. The result agrees well with the finding that DYRK1A(N) without the kinase domain bound to WDR68 as shown in Fig. 5 B & C.

3.5. WD40 repeats are not sufficient for the binding of WDR68 to DYRK1A

As WD40 domains are often responsible for protein-protein interactions, we speculated that one or several WD40 domain(s) among five WD40 repeats in WDR68 might be responsible for the binding to DYRK1A. We made deletion mutants of WDR68 as shown in Fig. 6A and examined their DYRK1A-binding capacity by co-immunoprecipitation experiments. Full length wild type WDR68 was co-immunoprecipitated with DYRK1A (Fig. 6B, *upper panel*, *lane* 4). To our surprise, the five WD40 repeats (amino acids 55-304) were not sufficient to support the DYRK1A-binding (Fig. 6B, *upper panel*, *lane* 8), and a deletion in either the N-terminal (amino acids 55-342, *lane* 11) or the C-terminal (amino acids 1-304, *lane* 7) region completely abolished the association of WDR68 with DYRK1A. The amounts of expressed DYRK1A did not change (Fig. 6B, *middle panel, lanes* 3-11) and sufficient levels of all WDR68 mutants were expressed with expected molecular masses (Fig. 6B, *lower panel, lanes 4-11, arrows*). We therefore concluded that the five WD40 domains of WDR68 are not sufficient for the binding to DYRK1A. Rather, a stretch in both the N-terminal and C-terminal regions of the molecule, or a complete molecular architecture of WDR68, is essential for its binding to DYRK1A.

3.6. Nuclear translocation of WDR68 by DYRK1A binding

We examined the intracellular distribution of WDR68 by immunofluorescent microscopic analysis. Staining with the anti-WDR68 antibody revealed that endogenous WDR68 was distributed throughout the cell (Fig. 7B, *green*). We observed only very faint staining by the same concentration of control IgG (Fig. 7A), indicating the specific staining of endogenous WDR68 with the antibody. Interestingly, cytoplasmic staining was stronger than nuclear WDR68 in some cells, while in other cells the staining was predominant in the nucleus, suggesting a dynamic shuttling of WDR68 between the cytoplasm and the nucleus. We then examined if the association with DYRK1A affects the intracellular distribution of WDR68. GFP-WDR68 was expressed in cells with 3×FLAG-DYRK1A or alone, and the cellular distribution of WDR68 and DYRK1A was examined by GFP fluorescence and anti-FLAG immunostaining, respectively. GFP-WDR68 was distributed throughout the cell (Fig. 8C, *green*) as endogenous WDR68 (Fig. 7). In agreement with previous reports, overexpressed DYRK1A was present exclusively in the nucleus (Fig. 8B, *magenta*). Interestingly in the presence of co-expressed DYRK1A, WDR68 was predominantly present in the nucleus (Fig. 8D, *green*) and was co-localized with DYRK1A (Fig. 8D, *merged images*). The nuclear translocation of WDR68 induced by DYRK1A was independent of the kinase activity of DYRK1A, because a kinase inactive mutant of DYRK1A, DYRK1A(KD), also induced nuclear translocation of WDR68 as wild type DYRK1A (Fig. 8E). In a reverse-tag experiments, we also observed that 3×FLAG-WDR68 became almost exclusively nuclear in the presence of co-expressed GFP-DYRK1A and was co-localized with DYRK1A in the nucleus (data not shown). The N-terminal domain of DYRK1A contains a bipartite nuclear localization signal [4, 41] and our results indicated that the domain is responsible for the WDR68-binding (Fig. 5). As shown in Fig. 8F, the N-terminal domain of DYRK1A was distributed exclusively in the nucleus (*magenta*), and it alone induced the nuclear accumulation of WDR68

(*green*). By contrast, DYRK1A(K+C) lacks the nuclear localization signal in the N-terminal domain, and did not accumulate in the nucleus (Fig. 8G, *magenta*). In addition, DYRK1A(K+C) did not interact with WDR68 as shown in Fig. 5C. Accordingly, the cellular distribution of WDR68 remained unchanged by DYRK1A(K+C) overexpression (Fig. 8G, green) and WDR68 did not co-localize with DYRK1A(K+C) (Fig. 8G, *merged images*). The subcellular localization of DYRK1A was not affected by the co-expression of WDR68 (Fig. 8).

Finally, we examined if overexpression of DYRK1A induces nuclear accumulation of endogenous WDR68. COS7 cells were transfected either with a control plasmid (Fig. 9A) or with plasmid encoding 3×FLAG-DYRK1A(WT) (Fig. 9B), and the subcellular distribution of endogenous WDR68 was examined by immunofluorescent microscopy. Strong nuclear accumulation of endogenous WDR68 was observed only in cells overexpressing DYRK1A (Fig. 9B, *green, white arrow heads*), whereas the distribution of WDR68 in other cells in the same microscopic field remained unchanged. We noticed that WDR68 did not accumulate in the nucleus in some of DYRK1A-overexpressing cells, suggesting an additional factor that controls the subcellular localization of endogenous WDR68. Taken together, all of these results shown in Fig. 8 and Fig. 9 indicate that DYRK1A binds to WDR68 and induces nuclear accumulation of WDR68 in a phosphorylation-independent manner, and WDR68 exists in the nucleus as complexes with DYRK1A.

4. Discussion

4.1. The binding of WDR68 to DYRK1A and DYRK1B

In this paper, we identified WDR68 as a DYRK1A binding protein and analyzed the association between WDR68 and DYRK1A in detail. In addition, the physiological importance of WDR68 for

cell proliferation and survival was established. Our results are in good agreement with and further extend two previous reports that implicated a functional relationship between WDR68 and DYRK1A as described in Introduction [16, 31]. During this study, a physical association between WDR68 and DYRK1B of zebrafish in an *in vitro* translational assay [42] and a scaffold function of Han11 (WDR68) for MEKK1 and DYRK1A·HIPK2 [43] have been reported. All of these observations can well be explained by our present finding showing that WDR68 binds to the N-terminal domain of DYRK1A and DYRK1B, which is not well conserved in DYRK2, DYRK3, or DYRK4. It should be natural to consider that WDR68 and DYRK1A·DYRK1B constitute a multi-facet complex regulating many cellular functions.

4.2. Subcellular localization and physiological function of WDR68

Our siRNA results demonstrated that mammalian cells can not grow or survive without WDR68 (Fig. 2). WDR68 suppression induced cell rounding and floating in the medium, with concomitant induction of cell apoptosis as indicated by the accumulation of caspase-cleaved PARP (Fig. 2D), and most cells died 5 days after introduction of WDR68-targeting siRNAs. The cell death caused by WDR68 suppression could not be rescued by concomitant overexpression of DYRK1A (data not shown), suggesting that DYRK1A is not a sole functional target of WDR68. The amino acid sequences of WDR68 are highly conserved among species, and WDR68 might therefore function in a fundamental biological process essential for many species from plants to human. WDR68 is crucial for expression of anthocyanin synthetic enzymes in plant [26, 44] and plays an important function in craniofacial development in zebrafish [45], suggesting a possible role for WDR68 in regulating gene expression. However, the molecular basis why such diverged physiological functions could be ascribed to WDR68 remains elusive.

GFP-tagged zebrafish WDR68 was reported to be in the nucleus when expressed in 293 cells [45], whereas petunia WDR68 was shown to be cytosolic by fractionation experiments [26]. HA-tagged human WDR68 was reported to be present in both the nucleus and cytoplasm in transfected 293T cells [31]. In this study, our results demonstrate for the first time that endogenous WDR68 exists throughout the cells by immunofluorescence staining (Fig. 7 & 9). WDR68 should have a role and specific partners both in the cytoplasm and the nucleus. We showed that overexpression of DYRK1A induced translocation of WDR68 into the cell nucleus where WDR68 was co-localized with DYRK1A (Fig. 8 & 9). In addition, we observed the physical association (Fig. 5D) and nuclear accumulation (Fig. 8) of WDR68 with a kinase-dead mutant of DYRK1A, therefore, the binding, but not the phosphorylation event, might induce the nuclear accumulation of WDR68 by DYRK1A. This suggests that DYRK1A recruits WDR68 into the nucleus by the association, or that DYRK1A might function as a nuclear anchoring protein for WDR68.

4.3. The WDR68-binding site in DYRK1A

DYRK1A is composed of the N-terminal domain, the central protein kinase catalytic domain, and the C-terminal domain. Analyses with deletion mutants showed that the N-terminal domain is the WDR68-binding site (Fig. 5). One of two nuclear localization signals of DYRK1A was mapped within the N-terminal region [2, 41], but no other function has been ascribed to the N-terminal domain. We showed that the DYRK1A N-terminal domain alone was localized in the nucleus and induced the nuclear accumulation of WDR68 upon co-expression (Fig. 8F). Five members of the DYRK kinases share a high degree of conservation in the catalytic domain, but are divergent in their N- and C-terminal domains. Our results show that DYRK1A and DYRK1B, but not DYRK2, DYRK3, or DYRK4, bound to WDR68 (Fig. 4). Indeed, a part of the N-terminal domain of DYRK1A shows

71% identity with that of DYRK1B (see Fig. 5), suggesting that this region is the WDR68-binding site within both DYRK1A and DYRK1B. Overexpression of WDR68 did not influence tyrosine phosphorylation or kinase activity of DYRK1A (data not shown), suggesting that the binding of WDR68 is not involved in the folding process or the catalytic regulation of DYRK1A. Therefore, WDR68 might not function as a direct activator or suppressor of DYRKs. However, we cannot rule out a possibility that abundant endogenous WDR68 is sufficient for supporting DYRK1A and DYRK1B.

4.4. The DYRK1A-binding activity and WD40 repeats of WDR68

WDR68 contains five sets of WD40 domains (Fig. 6). WD40 repeating units are believed to serve as a scaffold for simultaneous interactions with different proteins [28, 29, 46]. Crystal structures of several WD40 proteins, including signal-transducing heterotrimeric G protein β [47, 48], SCF^{Fbw7} ubiquitin ligase [49], and RACK1 [50, 51] have been determined. Most WD40 proteins consist of 7 WD-repeats and fold into a 7-bladed β-propeller structure. Our results demonstrate that the five WD40 repeats *per se* are not sufficient for the DYRK1A interaction (Fig. 6). The N-terminal and C-terminal domains might form together a DYRK1A binding site, while WD40 repeats might be responsible for the binding to other proteins. Most known propeller ring proteins appear to have some mechanism for holding the ring closed [28]. The N-terminal and C-terminal extensions thus might function to keep a possible 5-bladed propeller structure of WDR68 stabilized and closed. Coronin-1 forms a 7-bladed β-propeller composed of its five WD40 repeats and two additional blades encoded in a sequence that lacks any homology to the canonical WD40 motif [52]. Similarly, WDR68 may form a 7-bladed β-propeller structure that requires the N-terminal and C-terminal extensions for two blades in addition to the five WD40 blades. Structural analysis of WDR68 will

shed light on the interaction with DYRK1A at a molecular level.

4.5. Down's syndrome and DYRK1A

Down's syndrome, the most common genetic disorder leading to mental retardation with neurodevelopmental abnormalities, is caused by the presence of all or a part of triplicated chromosome 21. DYRK1A is encoded in the most critical region (21q-22) [6, 7], and transgenic mice overexpressing DYRK1A exhibit hyperactivity and impaired neuromotor development as well as learning and memory defects [8, 9, 53]. Many of these phenotypes are recovered by normalizing DYRK1A protein levels with DYRK1A-targeting siRNA [54]. Aberrant overexpression of DYRK1A in trisomy 21 carriers should therefore contribute to mental retardation and other developmental disorders. In this report, we found that overexpression of DYRK1A induced nuclear translocation of WDR68 in a kinase-activity independent manner (Fig. 8 & 9). WDR68 regulates gene expression [26, 42, 45], so the binding of overexpressed DYRK1A to WDR68 in the nucleus might induce aberrant gene expression. This could be a part of mechanism that DYRK1A overexpression induces pleiotropic phenotypes observed in Down's syndrome patient. The specific facial features are among the characteristics of Down's syndrome, and an important role in craniofacial development was suggested for DYRK1A using mouse model [13] and also for WDR68 by zebrafish screening [45], further supporting our hypothesis that DYRK1A and WDR68 should cooperatively work in cells. Although there should be additional mechanism to control the function and the subcellular distribution of WDR68, our results suggest the functional and physiological importance of the binding between DYRK1A and WDR68 to understand the biology of Down's syndrome and to unveil cellular functions of DYRK1A and WDR68 at the molecular level. Recently, specific inhibitors against DYRK1A [55] and a WD40 protein $Cdc4^{SCF}$ [56] were reported. Inhibition of DYRK1A and/or WDR68 by

low-molecular weight compounds can be a possible way to suppress multiple outcomes caused by DYRK1A overexpression in cells and in human bodies.

4.6. Conclusions

We identified WDR68, an evolutionarily conserved WD40-protein, as a cellular binding partner of DYRK1A. WDR68 was indispensable for the optimal proliferation and survival of mammalian cells. DYRK1A and DYRK1B, but not DYRK2, DYRK3, or DYRK4, bound to WDR68. The N-terminal domain, but not the catalytic kinase domain or the C-terminal domain of DYRK1A, was responsible for the WDR68 binding. WDR68 was distributed throughout the cell, and overexpression of DYRK1A resulted in nuclear accumulation of WDR68 in a kinase activity-independent manner. These results suggest that DYRK1A binds specifically to WDR68 in cells, thereby inducing nuclear translocation of WDR68. The binding of overexpressed DYRK1A to WDR68 in the nucleus might be a part of the molecular mechanism underlying the pleiotropic pathological alterations observed in Down's syndrome patient.

Acknowledgments

We would like to give our thanks to T. Sakabe, T. Aoki, and M. Nakagawa for their excellent technical assistance. This work was supported by Grants-in-Aid for Scientific Research from the Ministry of Education, Culture, Sports, Science and Technology of Japan.

References

[1] W. Becker, H.-G. Joost, Structural and functional characteristics of Dyrk, a novel subfamily of protein kinases with dual specificity, Prog. Nucleic Acid Res. Mol. Biol. 62 (1999) 1-17.

[2] W. Becker, Y. Weber, K. Wetzel, K. Eirmbter, F.J. Tejedor, H.-G. Joost, Sequence characteristics, subcellular localization, and substrate specificity of DYRK-related kinases, a novel family of dual specificity protein kinases, J. Biol. Chem. 273 (1998) 25893-25902.

[3] Y. Miyata, E. Nishida, Distantly related cousins of MAP kinase: Biochemical properties and possible physiological functions, Biochem. Biophys. Res. Commun. 266 (1999) 291-295.

[4] H. Kentrup, W. Becker, J. Heukelbach, A. Wilmes, A. Schürmann, C. Huppertz, H. Kainulainen, H.-G. Joost, Dyrk, a dual specificity protein kinase with unique structural features whose activity is dependent on tyrosine residues between subdomain VII and VIII, J. Biol. Chem. 271 (1996) 3488-3495.

[5] P.A. Lochhead, G. Sibbet, N. Morrice, V. Cleghon, Activation-loop autophosphorylation is mediated by a novel transitional intermediate form of DYRKs, Cell 121 (2005) 925-936.

[6] J. Galceran, K. de Graaf, F.J. Tejedor, W. Becker, The Mnb/Dyrk1A protein kinase: genetic and biochemical properties, J. Neural Transm. 67 (2003) 139-148.

[7] B. Hämmerle, C. Elizalde, J. Galceran, W. Becker, F.J. Tejedor, The Mnb/Dyrk1A protein kinase: neurobiological functions and Down syndrome implications, J. Neural Transm. 67 (2003) 129-137.

[8] X. Altafaj, M. Dierssen, C. Baamonde, E. Martí, J. Visa, J. Guimerà, M. Oset, J.R. González, J. Flórez, C. Fillat, X. Estivill, Neurodevelopmental delay, motor abnormalities and cognitive deficits in transgenic mice overexpressing *Dyrk1A* (*minibrain*), a murine model of Down's syndrome, Hum. Mol. Genet. 10 (2001) 1915-1923.

[9] M. Martínez de Lagrán, X. Altafaj, X. Gallego, E. Martí, X. Estivill, I. Sahún, C. Fillat, M. Dierssen, Motor phenotypic alterations in TgDyrk1a transgenic mice implicate DYRK1A in Down syndrome motor dysfunction, Neurobiol. Dis. 15 (2004) 132-142.

[10] J. Park, E.J. Yang, J.H. Yoon, K.C. Chung, Dyrk1A overexpression in immortalized hippocampal cells produces the neuropathological features of Down syndrome, Mol. Cell. Neurosci. 36 (2007) 270-279.

[11] F. Liu, Z. Liang, J. Wegiel, Y.W. Hwang, K. Iqbal, I. Grundke-Iqbal, N. Ramakrishna, C.X. Gong, Overexpression of Dyrk1A contributes to neurofibrillary degeneration in Down syndrome, FASEB J. 22 (2008) 3224-3233.

[12] O. Yabut, J. Domogauer, G. D'Arcangelo, Dyrk1A overexpression inhibits proliferation and induces premature neuronal differentiation of neural progenitor cells, J. Neurosci. 30 (2010) 4004-4014.

[13] J.R. Arron, M.M. Winslow, A. Polleri, C.P. Chang, H. Wu, X. Gao, J.R. Neilson, L. Chen, J.J. Heit, S.K. Kim, N. Yamasaki, T. Miyakawa, U. Francke, I.A. Graef, G.R. Crabtree, NFAT dysregulation by increased dosage of DSCR1 and DYRK1A on chromosome 21, Nature 441 (2006) 595-600.

[14] Y. Gwack, S. Sharma, J. Nardone, B. Tanasa, A. Iuga, S. Srikanth, H. Okamura, D. Bolton, S. Feske, P.G. Hogan, A. Rao, A genome-wide *Drosophila* RNAi screen identifies DYRK-family kinases as regulators of NFAT, Nature 441 (2006) 646-650.

[15] S.R. Ryoo, H.K. Jeong, C. Radnaabazar, J.J. Yoo, H.J. Cho, H.W. Lee, I.S. Kim, Y.H. Cheon, Y.S. Ahn, S.H. Chung, W.J. Song, DYRK1A-mediated hyperphosphorylation of Tau. A

functional link between Down syndrome and Alzheimer disease, J. Biol. Chem. 282 (2007) 34850-34857.

[16] A.V. Skurat, A.D. Dietrich, Phosphorylation of Ser640 in muscle glycogen synthase by DYRK family protein kinases, J. Biol. Chem. 279 (2004) 2490-2498.

[17] N. Kurabayashi, T. Hirota, M. Sakai, K. Sanada, Y. Fukada, DYRK1A and glycogen synthase kinase 3β, a dual-kinase mechanism directing proteasomal degradation of CRY2 for circadian timekeeping, Mol. Cell. Biol. 30 (2010) 1757-1768.

[18] A. Laguna, S. Aranda, M.J. Barallobre, R. Barhoum, E. Fernandez, V. Fotaki, J.M. Delabar, S. de la Luna, P. de la Villa, M.L. Arbones, The protein kinase DYRK1A regulates caspase-9-mediated apoptosis during retina development, Dev. Cell 15 (2008) 841-853.

[19] A. Seifert, L.A. Allan, P.R. Clarke, DYRK1A phosphorylates caspase 9 at an inhibitory site and is potently inhibited in human cells by harmine, FEBS J. 275 (2008) 6268-6280.

[20] S. Leder, Y. Weber, X. Altafaj, X. Estivill, H.G. Joost, W. Becker, Cloning and characterization of DYRK1B, a novel member of the DYRK family of protein kinases, Biochem. Biophys. Res. Commun. 254 (1999) 474-479.

[21] S.E. Mercer, E. Friedman, Mirk/Dyrk1B: a multifunctional dual-specificity kinase involved in growth arrest, differentiation, and cell survival, Cell Biochem. Biophys. 45 (2006) 303-315.

[22] S.E. Mercer, D.Z. Ewton, X. Deng, S. Lim, T.R. Mazur, E. Friedman, Mirk/Dyrk1B mediates survival during the differentiation of C2C12 myoblasts, J. Biol. Chem. 280 (2005) 25788-25801.

[23] J. Gao, Z. Zheng, B. Rawal, M.J. Schell, G. Bepler, E.B. Haura, Mirk/Dyrk1B, a novel therapeutic target, mediates cell survival in non-small cell lung cancer cells, Cancer Biol. Ther. 8 (2009) 1671-1679.

[24] K. Jin, S. Park, D.Z. Ewton, E. Friedman, The survival kinase Mirk/Dyrk1B is a downstream effector of oncogenic K-ras in pancreatic cancer, Cancer Res. 67 (2007) 7247-7255.

[25] M. Lauth, A. Bergstrom, T. Shimokawa, U. Tostar, Q. Jin, V. Fendrich, C. Guerra, M. Barbacid, R. Toftgard, DYRK1B-dependent autocrine-to-paracrine shift of Hedgehog signaling by mutant RAS, Nat. Struct. Mol. Biol. 17 (2010) 718-725.

[26] N. de Vetten, R.M. Nissen, J. Mol, R. Koes, The an11 locus controlling flower pigmentation in petunia encodes a novel WD-repeat protein conserved in yeast, plants, and animals, Genes Dev. 11 (1997) 1422-1434.

[27] J. Jin, E.E. Arias, J. Chen, J.W. Harper, J.C. Walter, A family of diverse Cul4-Ddb1-interacting proteins includes Cdt2, which is required for S phase destruction of the replication factor Cdt1, Mol. Cell 23 (2006) 709-721.

[28] T.F. Smith, C. Gaitatzes, K. Saxena, E.J. Neer, The WD repeat: a common architecture for diverse functions, Trends Biochem. Sci. 24 (1999) 181-185.

[29] D. Li, R. Roberts, WD-repeat proteins: structure characteristics, biological function, and their involvement in human diseases, Cell. Mol. Life Sci. 58 (2001) 2058-2097.

[30] J. Mao, P. Maye, P. Kogerman, F.J. Tejedor, R. Toftgard, W. Xie, G. Wu, D. Wu, Regulation of Gli1 transcriptional activity in the nucleus by Dyrk1, J. Biol. Chem. 277 (2002) 35156-35161.

[31] K. Morita, C. Lo Celso, B. Spencer-Dene, C.C. Zouboulis, F.M. Watt, HAN11 binds mDia1 and controls GLI1 transcriptional activity, J. Dermatol. Sci. 44 (2006) 11-20.

[32] S. Koyasu, E. Nishida, T. Kadowaki, F. Matsuzaki, K. Iida, F. Harada, M. Kasuga, H. Sakai, I. Yahara, Two mammalian heat shock proteins, HSP90 and HSP100, are actin-binding proteins, Proc. Natl. Acad. Sci. USA. 83 (1986) 8054-8058.

[33] Y. Miyata, I. Yahara, p53-independent association between SV40 large T antigen and the major cytosolic heat shock protein, HSP90, Oncogene 19 (2000) 1477-1484.

[34] Y. Miyata, B. Chambraud, C. Radanyi, J. Leclerc, M.-C. Lebeau, J.-M. Renoir, R. Shirai, M.-G. Catelli, I. Yahara, E.-E. Baulieu, Phosphorylation of the immunosuppressant FK506-binding protein FKBP52 by casein kinase II (CK2): Regulation of HSP90-binding activity of FKBP52, Proc. Natl. Acad. Sci. USA. 94 (1997) 14500-14505.

[35] Y. Miyata, M. Akashi, E. Nishida, Molecular cloning and characterization of a novel member of the MAP kinase superfamily, Genes Cells 4 (1999) 299-309.

[36] Y. Miyata, Y. Ikawa, M. Shibuya, E. Nishida, Specific association of a set of molecular chaperones including HSP90 and Cdc37 with MOK, a member of the MAP kinase superfamily, J. Biol. Chem. 276 (2001) 21841-21848.

[37] Y. Miyata, E. Nishida, CK2 controls multiple protein kinases by phosphorylating a kinase-targeting molecular chaperone Cdc37, Mol. Cell. Biol. 24 (2004) 4065-4074.

[38] Y. Miyata, E. Nishida, CK2 binds, phosphorylates, and regulates its pivotal substrate Cdc37, an Hsp90-cochaperone, Mol. Cell. Biochem. 274 (2005) 171-179.

[39] D.W. Nicholson, A. Ali, N.A. Thornberry, J.P. Vaillancourt, C.K. Ding, M. Gallant, Y. Gareau, P.R. Griffin, M. Labelle, Y.A. Lazebnik, N.A. Munday, S.M. Raju, M.E. Smulson, T.-T. Yamin, V.L. Yu, D.K. Miller, Identification and inhibition of the ICE/CED-3 protease necessary for mammalian apoptosis, Nature 376 (1995) 37-43.

[40] M. Tewari, L.T. Quan, K. O'Rourke, S. Desnoyers, Z. Zeng, D.R. Beidler, G.G. Poirier, G.S. Salvesen, V.M. Dixit, Yama/CPP32β, a mammalian homolog of CED-3, is a CrmA-inhibitable protease that cleaves the death substrate poly(ADP-ribose) polymerase, Cell 81 (1995) 801-809.

[41] M. Alvarez, X. Estivill, S. de la Luna, DYRK1A accumulates in splicing speckles through a novel targeting signal and induces speckle disassembly, J. Cell Sci. 116 (2003) 3099-3107.

[42] G. Mazmanian, M. Kovshilovsky, D. Yen, A. Mohanty, S. Mohanty, A. Nee, R.M. Nissen, The zebrafish dyrk1b gene is important for endoderm formation, Genesis 48 (2010) 20-30.

[43] S. Ritterhoff, C.M. Farah, J. Grabitzki, G. Lochnit, A.V. Skurat, M.L. Schmitz, The WD40-repeat protein Han11 functions as a scaffold protein to control HIPK2 and MEKK1 kinase functions, EMBO J. 29 (2010) 3750-3761.

[44] A.R. Walker, P.A. Davison, A.C. Bolognesi-Winfield, C.M. James, N. Srinivasan, T.L. Blundell, J.J. Esch, M.D. Marks, J.C. Gray, The TRANSPARENT TESTA GLABRA1 locus, which regulates trichome differentiation and anthocyanin biosynthesis in Arabidopsis, encodes a WD40 repeat protein, Plant Cell 11 (1999) 1337-1350.

[45] R.M. Nissen, A. Amsterdam, N. Hopkins, A zebrafish screen for craniofacial mutants identifies wdr68 as a highly conserved gene required for endothelin-1 expression, BMC Dev. Biol. 6 (2006) 28-44.

[46] L. van der Voorn, H.L. Ploegh, The WD-40 repeat, FEBS J. 307 (1992) 131-134.

[47] M.A. Wall, D.E. Coleman, E. Lee, J.A. Iñiguez-Lluhi, B.A. Posner, A.G. Gilman, S.R. Sprang, The structure of the G protein heterotrimer $G_{i\alpha1}\beta_1\gamma_2$, Cell 83 (1995) 1047-1058.

[48] J. Sondek, A. Bohm, D.G. Lambright, H.E. Hamm, P.B. Sigler, Crystal structure of a G_A protein βγ {betagamma} dimer at 2.1Å resolution, Nature 379 (1996) 369-374.

[49] B. Hao, S. Oehlmann, M.E. Sowa, J.W. Harper, N.P. Pavletich, Structure of a Fbw7-Skp1-cyclin E complex: multisite-phosphorylated substrate recognition by SCF ubiquitin ligases, Mol. Cell 26 (2007) 131-143.

[50] S.M. Coyle, W.V. Gilbert, J.A. Doudna, Direct link between RACK1 function and localization at the ribosome in vivo, Mol. Cell. Biol. 29 (2009) 1626-1634.

[51] H. Ullah, E.L. Scappini, A.F. Moon, L.V. Williams, D.L. Armstrong, L.C. Pedersen, Structure of a signal transduction regulator, RACK1, from *Arabidopsis thaliana*, Protein Sci. 17 (2008)

1771-1780.

[52] B.A. Appleton, P. Wu, C. Wiesmann, The crystal structure of murine coronin-1: a regulator of actin cytoskeletal dynamics in lymphocytes, Structure 14 (2006) 87-96.

[53] K.J. Ahn, H.K. Jeong, H.S. Choi, S.R. Ryoo, Y.J. Kim, J.S. Goo, S.Y. Choi, J.S. Han, I. Ha, W.J. Song, DYRK1A BAC transgenic mice show altered synaptic plasticity with learning and memory defects, Neurobiol. Dis. 22 (2006) 463-472.

[54] J. Ortiz-Abalia, I. Sahún, X. Altafaj, N. Andreu, X. Estivill, M. Dierssen, C. Fillat, Targeting Dyrk1A with AAVshRNA attenuates motor alterations in TgDyrk1A, a mouse model of Down syndrome, Am. J. Hum. Genet. 83 (2008) 479-488.

[55] N. Göckler, G. Jofre, C. Papadopoulos, U. Soppa, F.J. Tejedor, W. Becker, Harmine specifically inhibits protein kinase DYRK1A and interferes with neurite formation, FEBS J. 276 (2009) 6324-6337.

[56] S. Orlicky, X. Tang, V. Neduva, N. Elowe, E.D. Brown, F. Sicheri, M. Tyers, An allosteric inhibitor of substrate recognition by the SCF^{Cdc4} ubiquitin ligase, Nat. Biotechnol. 28 (2010) 733-737.

Figure legends

Fig. 1. Isolation and identification of a cellular DYRK1A binding protein. (A) A silver staining pattern of complexes of DYRK1A with its associated proteins. 3×FLAG-DYRK1A was expressed in COS7 cells and isolated with its cellular binding partners using anti-FLAG affinity resin. The protein profile of the immunocomplexes was shown by silver staining. Lane 1, isolated from mock-transfected lysate; lane 2, isolated from 3×FLAG-DYRK1A expressing lysate. The positions of DYRK1A and its associated protein (arrow) are shown. (B) The amino acid sequence of human WDR68. The peptides identified by peptide mass spectrometry fingerprinting analysis of the 42 kDa protein band shown with an arrow in (A) are illustrated by boxes. (C) The reactivity of endogenous and expressed WDR68 to the anti-WDR68 antibody. Lane 1, untransfected cell lysate probed with preimmune serum; lane 2, 3×FLAG-WDR68-transfected cell lysate probed with preimmune serum; lane 3, untransfected cell lysate probed with the anti-WDR68 antibody; lane 4, 3×FLAG-WDR68-transfected cell lysate probed with the anti-WDR68 antibody. The positions of endogenous WDR68, 3×FLAG-WDR68, and molecular weight markers are shown.

Fig. 2. Effect of siRNA-induced suppression of endogenous WDR68 on the proliferation and apoptotic process of cultured cells. (A) COS7 (left) or KB (right) cells were transfected with control siRNA (lane 1), or two independent WDR68-specific siRNAs, RNAi-1 (lane 2, HSS145522) or RNAi-2 (lane 3, HSS145523). After 48 h, extracts were prepared from the same numbers of cells and the amounts of WDR68 (upper panels) or control proteins (left, Hsp90; right, Cdc37) were examined by western blotting with corresponding antibodies. (B) The numbers of living attached COS7 cells in 35-mm dishes were daily counted. Control (●), cells transfected with control siRNA;

RNAi-1 (▲), cells transfected with WDR68-specific RNA (HSS145522); RNAi-2 (■), cells transfected with WDR68-specific RNA (HSS145523). The control siRNA-transfected cells reached full confluency at day 3. (C) Two representative phase contrast photographs (upper and lower panels) of COS7 cells 2 days after siRNA introduction as described in (A) and (B) are shown. (D) Induction of cell apoptosis by WDR68 depletion. Effect of the two independent WDR68-specific siRNAs on the cleavage of an endogenous caspase substrate PARP was examined by western blotting analysis with an antibody specific for the cleaved form of PARP (upper panel). Lanes 1-4, control siRNA; lanes 5-8, RNAi-1; lanes 9-12, RNAi-2. The amount of Hsp90 was shown as a control (lower panel).

Fig. 3. Association between DYRK1A and WDR68. (A) The binding of DYRK1A to WDR68 was examined by co-immunoprecipitation experiments. COS7 cells were transfected with a control vector (lanes 1 & 4), a plasmid encoding 3×FLAG-DYRK1A (lanes 2 & 5) or co-transfected with 3×FLAG-DYRK1A and HA-WDR68 (lanes 3 & 6). 3×FLAG-DYRK1A was immunoprecipitated with anti-FLAG antibody (lanes 1-3). As controls, non-immune serum was used (lanes 4-6). The co-immunoprecipitation of WDR68 with DYRK1A was examined by western blotting with anti-HA antibody (upper panel). (B) The binding of DYRK1A to WDR68 was examined by reciprocal co-immunoprecipitation experiments. COS7 cells were transfected with a control vector (lane 1), a plasmid encoding 3×FLAG-WDR68 (lane 2) or co-transfected with 3×FLAG-WDR68 and HA-DYRK1A (lane 3). WDR68 was immunoprecipitated with anti-FLAG antibody, and the co-immunoprecipitation of DYRK1A with WDR68 was examined by western blotting with anti-HA antibody (upper panel). The amounts of expressed DYRK1A (middle panels) and WDR68 (lower panels) were examined by western blotting with anti-FLAG and anti-HA antibodies (A & B).

Asterisks indicate non-specific bands.

Fig. 4. Binding of DYRK1A and DYRK1B, but not DYRK2, DYRK3, or DYRK4, to WDR68. (A) The binding of 3×FLAG-tagged DYRK1A (lane 3), DYRK1B (lane 4), DYRK2 (lane 5), DYRK3 (lane 6), and DYRK4 (lane 7), to exogenously expressed HA-WDR68 was examined by co-transfection/co-immunoprecipitation experiments. The binding of WDR68 to immunoprecipitated 3×FLAG-DYRKs was revealed by western blotting with anti-HA antibody. (B) The binding of 3×FLAG-tagged DYRK1A (lane 2), DYRK1B (lane 3), DYRK2 (lane 4), DYRK3 (lane 5), and DYRK4 (lane 6) to endogenous WDR68 was examined by co-immunoprecipitation experiments. The binding of WDR68 was revealed by western blotting with the anti-WDR68 antibody. (C) The expression profiles of DYRK family protein kinases described in (B) were shown by western blotting with anti-FLAG antibody.

Fig. 5. The N-terminal domain of DYRK1A is responsible for the WDR68 binding. (A) A schematic illustration of the structure of DYRK1A and its deletion mutants used in the binding experiments. Alignment of the structures of DYRK1A and DYRK1B is also shown. The amino acid numbers of the beginnings and endings of domains are indicated. (B) The binding of DYRK1A(N) (lane 4), DYRK1A(K) (lane 5), and DYRK1A(C) (lane 6) to WDR68 was examined by co-transfection/co-immunoprecipitation experiments as described in Fig. 3A. (C) The binding of DYRK1A(N) (lane 3), DYRK1A(N+K) (lane 4), and DYRK1A(K+C) (lane 5) to WDR68 was examined by co-transfection/co-immunoprecipitation experiments as described in Fig. 3A. (D) The kinase activity of DYRK1A is not required for its binding to WDR68. The binding of DYRK1A(WT) (lane 3) and DYRK1A(KD) (lane 4) to WDR68 was examined by

co-transfection/co-immunoprecipitation experiments. In (B-D), the binding of WDR68 (upper panels), amounts of expressed and immunoprecipitated DYRK1A (middle panels), and amounts of expressed WDR68 (lower panels) are shown. Lane 1, control without transfection; lane 2, control with WDR68 transfection without DYRK1A transfection. Asterisks indicate non-specific bands.

Fig. 6. WD40 repeats of WDR68 are not sufficient for the binding to DYRK1A. (A) A schematic illustration of the structure of WDR68 and its deletion mutants used in the binding experiments. The amino acid numbers of the beginnings and endings of the five WD40 domains (shown as boxes) are indicated. (B) The binding of WDR68 mutants to DYRK1A. The WDR68 deletion mutants shown in (A) as indicated above the lane tracks were tested for their DYRK1A binding ability by co-immunoprecipitation experiments as described in Fig. 3A. The binding of WDR68 (upper panel), the amounts of DYRK1A (middle panel), and the expression of WDR68 deletion mutants (lower panel, indicated by arrows) are shown. An asterisk indicates a non-specific band.

Fig. 7. Intracellular localization of WDR68. Subcellular localization of endogenous WDR68 was examined by immunofluorescent microscopy in COS7 cells using affinity purified anti-WDR68 antibody (B). Staining with the same concentration of non-immune IgG was performed as a negative control (A). Two representative fluorescent images are shown (left, green) with phase contrast images (center) and nuclear images by Hoechst 33342 staining (right, blue).

Fig. 8. Nuclear translocation of WDR68 induced by DYRK1A binding. Intracellular localization of WDR68 and DYRK1A in transfected COS7 cells was visualized by fluorescent microscopy. Left column, the subcellular localization of WDR68 was shown by GFP fluorescence as green; 2nd left

column, the subcellular localization of DYRK1A was shown by anti-FLAG immunofluorescence as magenta; 3rd left column, the merged images of WDR68 and DYRK1A were shown, indicating co-localization as white; Right-most column, the corresponding phase contrast images were shown. Two representative images are shown for each sample. (A) Control cells; (B) Transfected with 3×FLAG-DYRK1A(WT); (C) Transfected with EGFP-WDR68; (D) Co-transfected with EGFP-WDR68 and 3×FLAG-DYRK1A(WT); (E) Co-transfected with EGFP-WDR68 and 3×FLAG-DYRK1A(KD); (F) Co-transfected with EGFP-WDR68 and 3×FLAG-DYRK1A(N); (G) Co-transfected with EGFP-WDR68 and 3×FLAG-DYRK1A(K+C).

Fig. 9. Nuclear accumulation of endogenous WDR68 by DYRK1A overexpression. Subcellular localization of endogenous WDR68 and expressed DYRK1A was examined by immunofluorescent microscopy using anti-WDR68 antibody and anti-FLAG antibody, respectively. (A) Transfected with a control vector; (B) Transfected with 3×FLAG-DYRK1A(WT) plasmid. Two representative fluorescent images for WDR68 (left, green) and DYRK1A (2nd left, magenta) are shown with nuclear images by Hoechst 33342 staining (3rd left, blue) and phase contrast images (right-most).

Figure 1 (Revised)

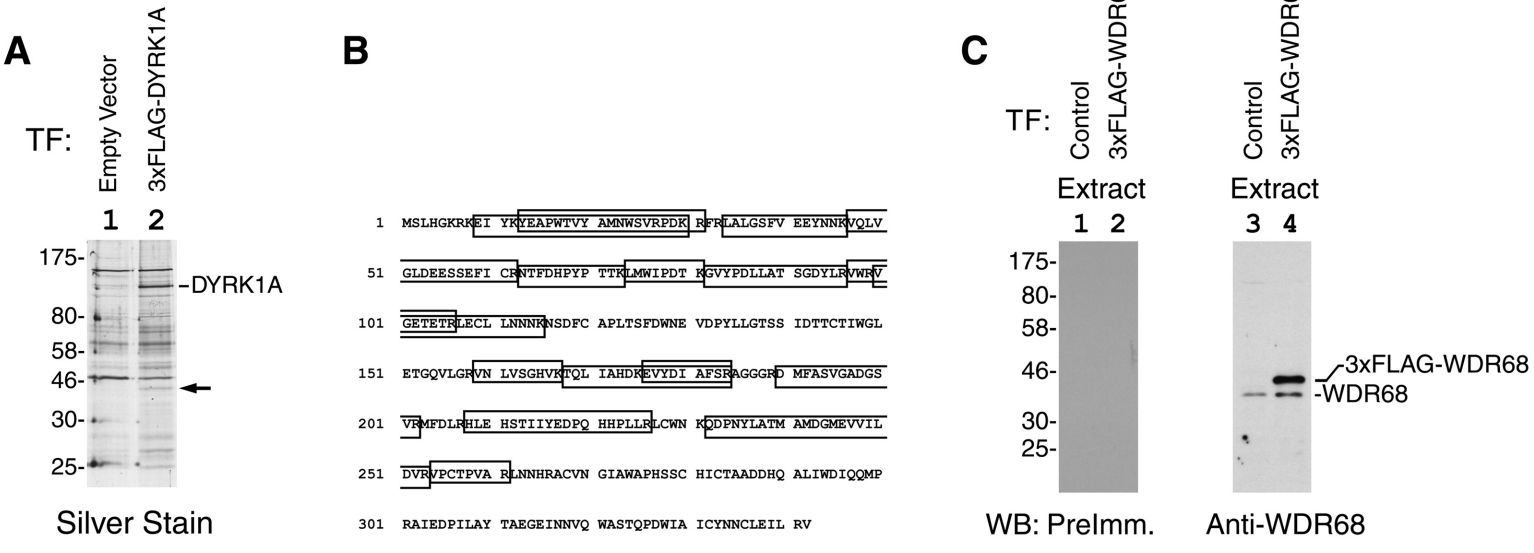

Figure 2 (Revised)

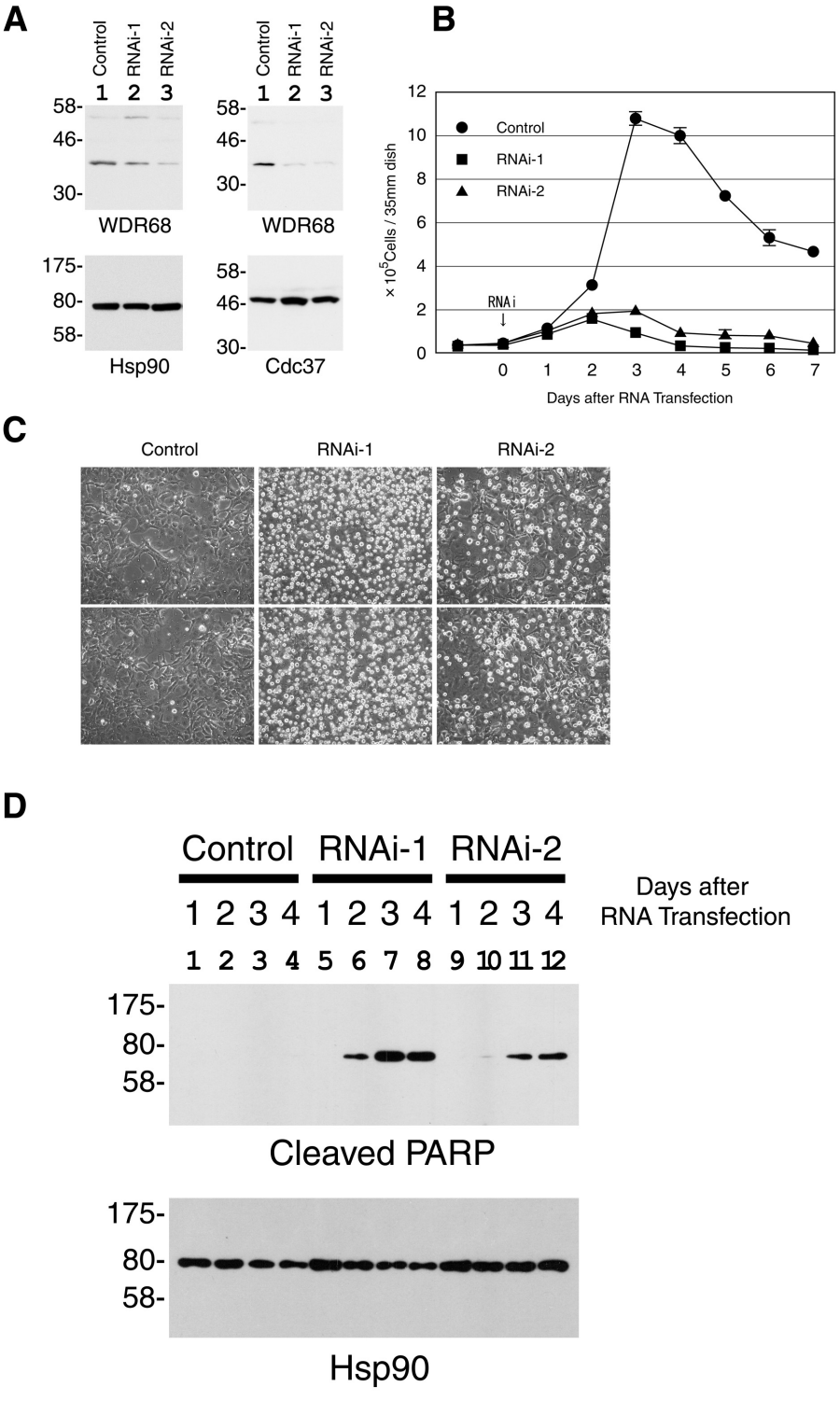

Figure 3 (Revised)

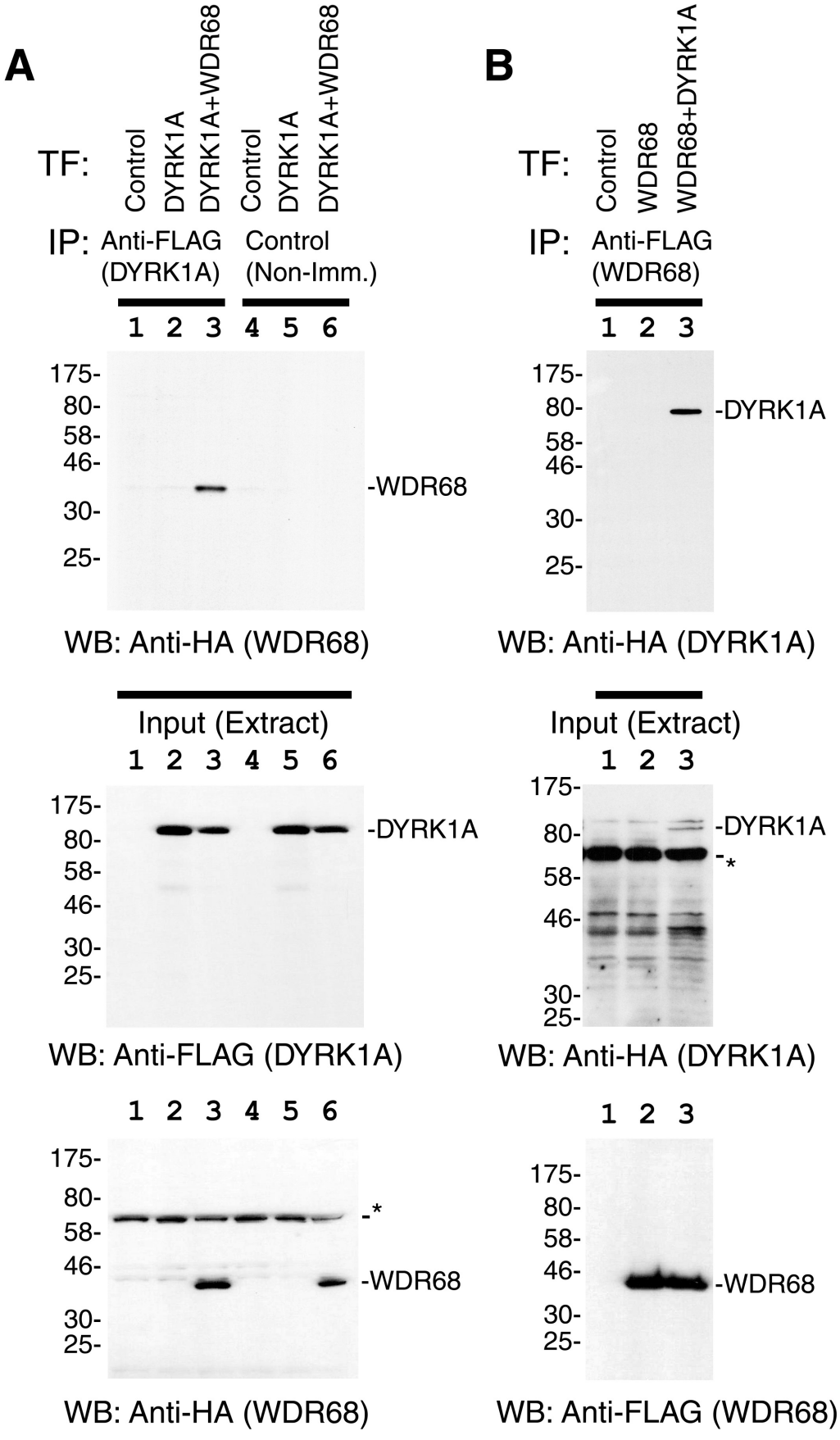

Figure 4 (Revised)

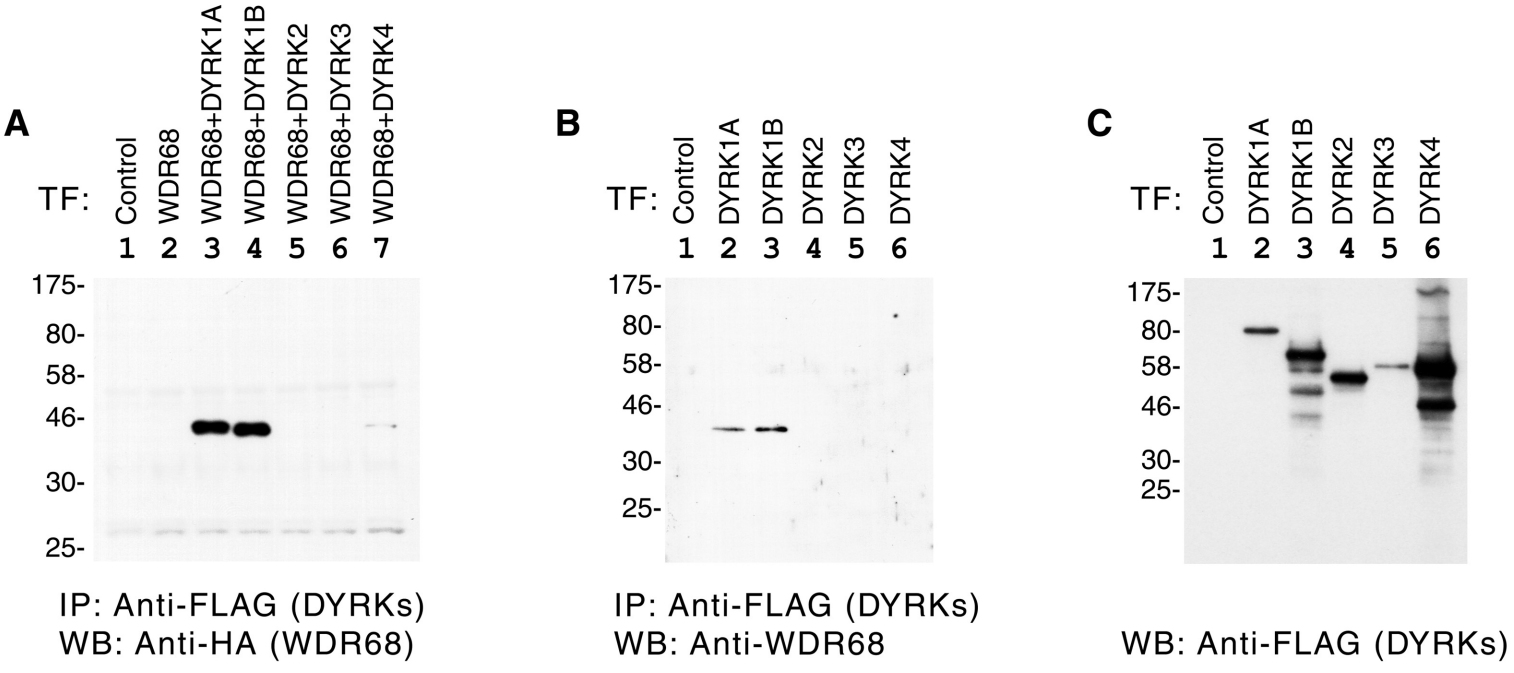

Figure 5 (Revised)

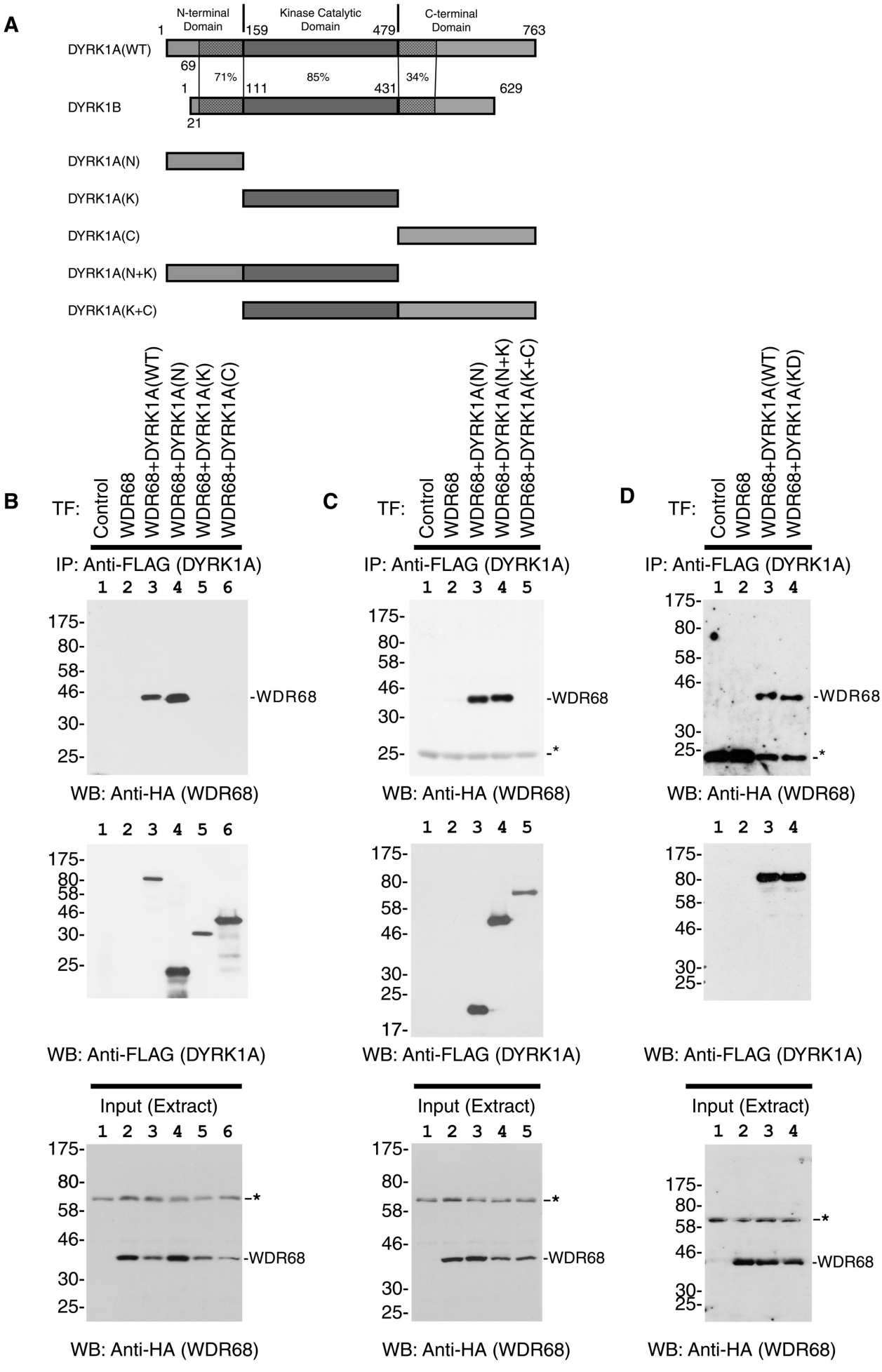

Figure 6 (Revised)

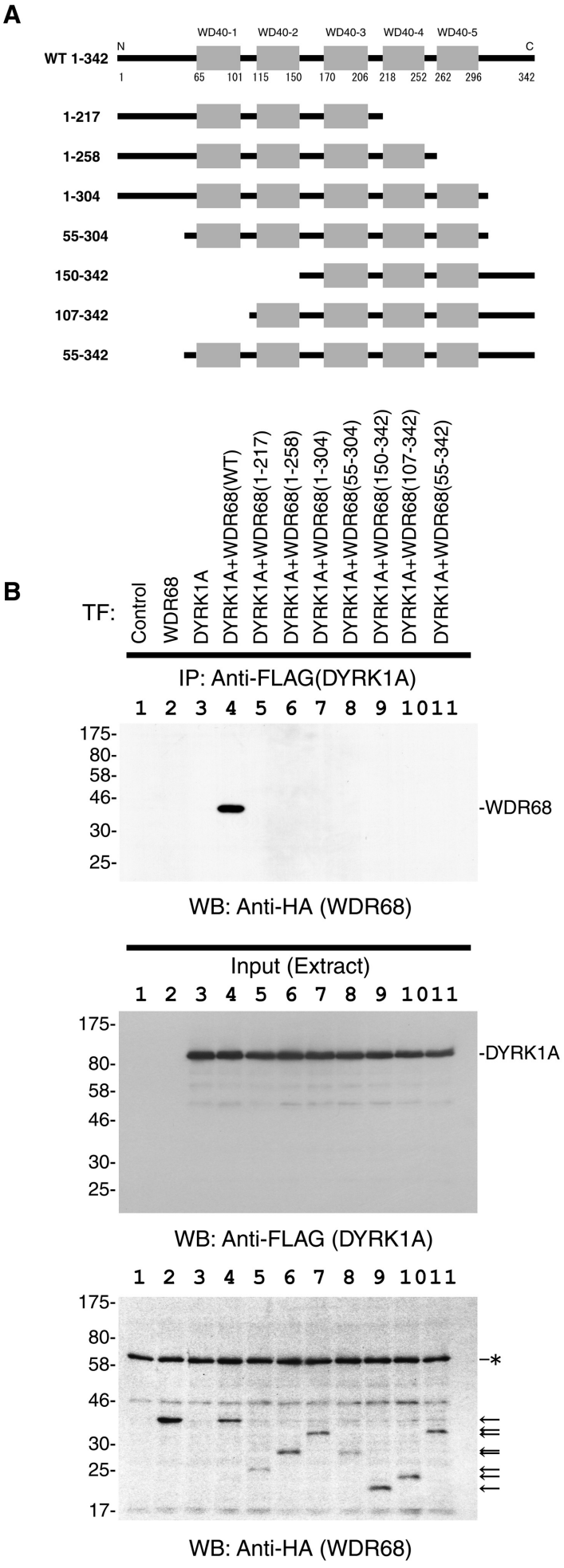

Figure 7 (Revised)

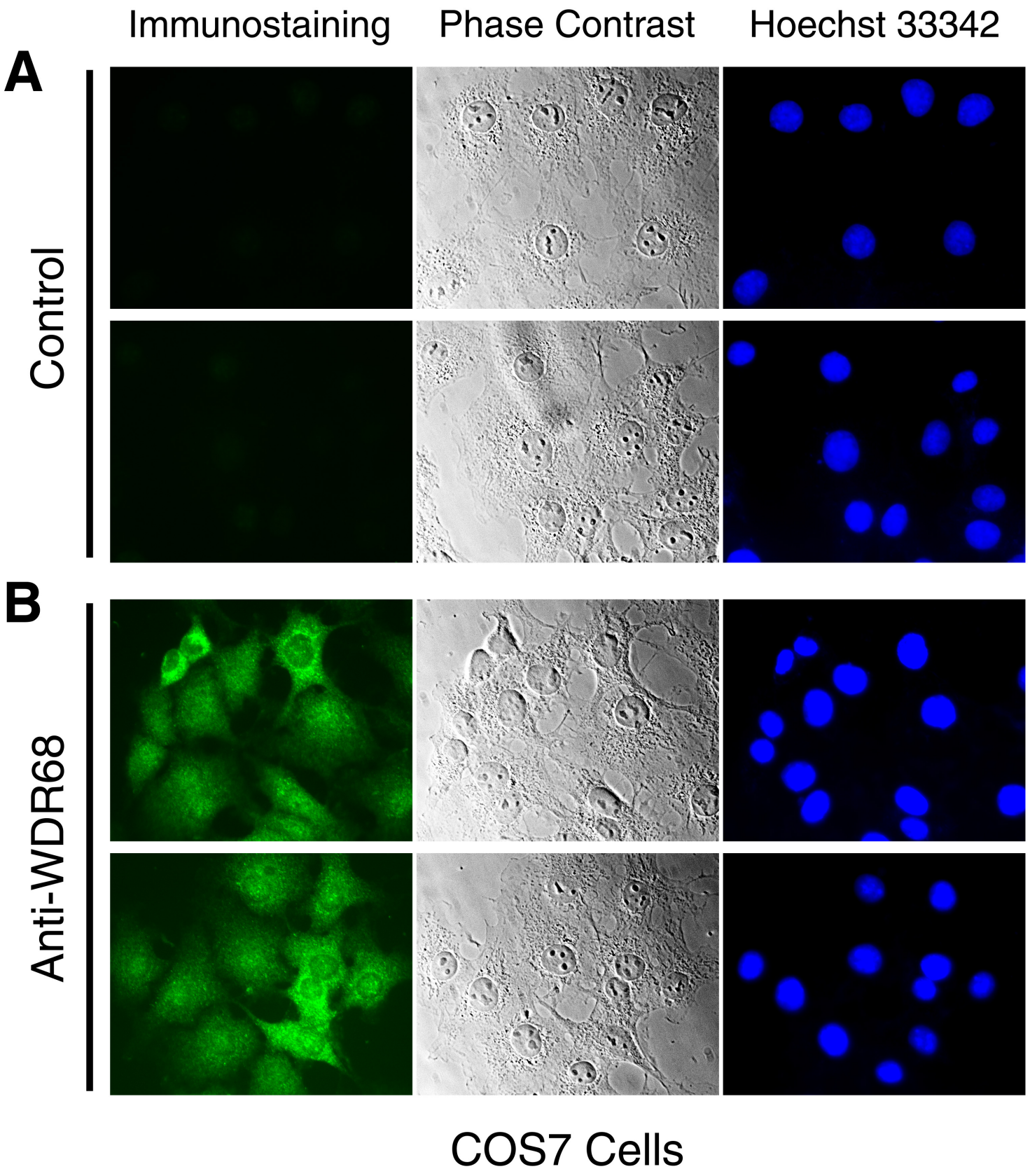

Figure 8 (Revised)

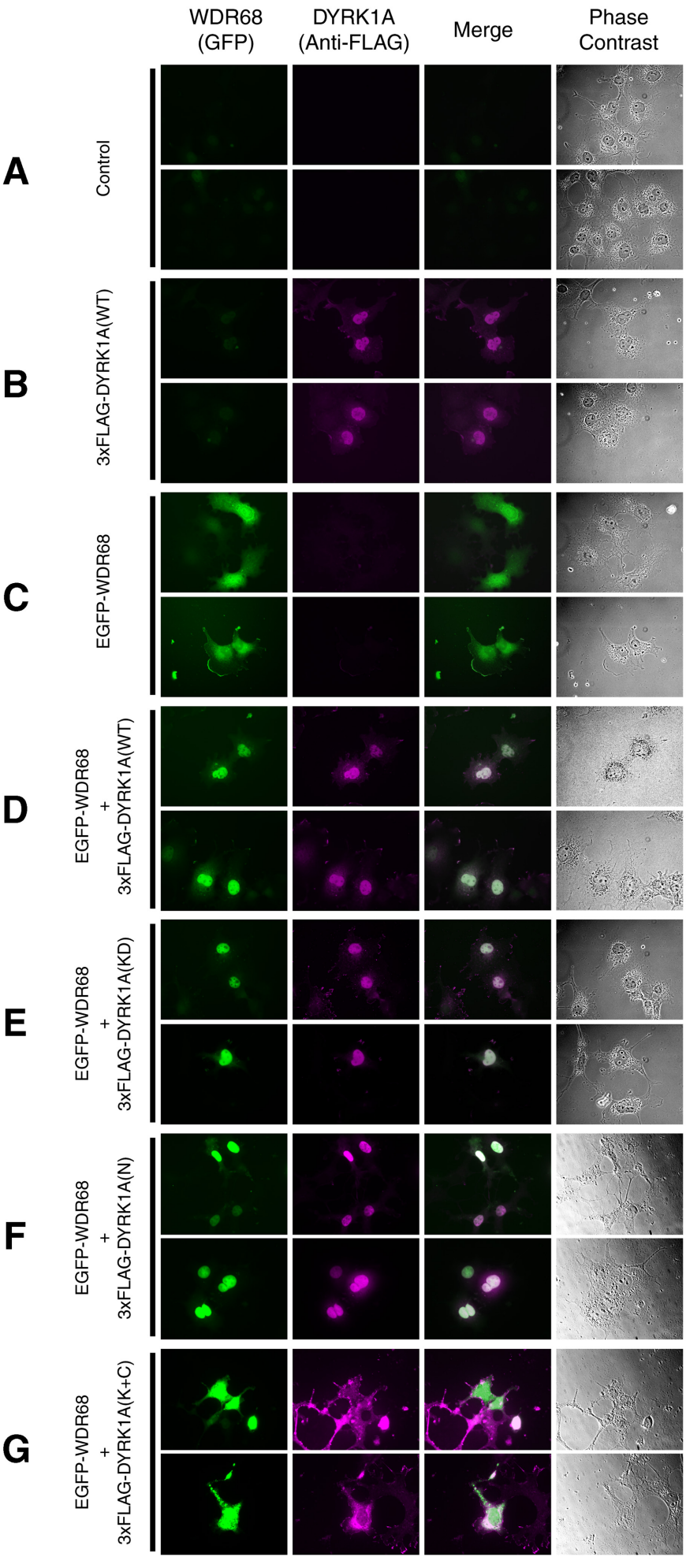

Figure 9 (Revised)